International Journal of Innovative
Computing, Information and Control
Volume **9**, Number **2**, February **2013**

 ISSN 1349-4198
pp. 465–475

WAVELET-COHERENCE FEATURES FOR MOTOR IMAGERY EEG ANALYSIS POSTERIOR TO EOG NOISE ELIMINATION

Wei-Yen Hsu[1,2]

[1]Department of Information Management
[2]Advanced Institute of Manufacturing with High-tech Innovations
National Chung Cheng University
No.168, Sec. 1, University Rd., Minhsiung Township, Chiayi County 621, Taiwan
shenswy@gmail.com

Received November 2011; revised March 2012

Abstract. *In this study, we propose a brain-computer interface (BCI) system to analyze single-trial electroencephalogram (EEG) signals. After the automatic EOG-artifact elimination, wavelet-coherence features and support vector machine (SVM) are adopted for the classification of left and right motor imagery (MI) data. EOG artifacts are removed automatically via modified independent component analysis (ICA). The features are extracted from wavelet data by means of coherence, and then classified by the SVM. Compared with EEG data without EOG artifact removal, spectral band and AR model features, the proposed system achieves satisfactory results in BCI applications.*
Keywords: Electroencephalogram (EEG), Brain-computer interface (BCI), Independent component analysis (ICA), Wavelet transform (WT), Coherence, Support vector machine (SVM)

1. **Introduction.** An alternative communication channel is provided for brain-computer interface (BCI) to transmit messages directly to computers by analyzing the brain's mental activities [1-6]. BCI systems based on single-trial electroencephalographic (EEG) signal analysis associated with finger movement have grown rapidly in the last decade [2]. It focuses on discriminating finger movements for EEG analysis using event-related brain potentials (ERP). It shows that there are special characteristics of event-related desynchronization (ERD) and synchronization (ERS) in mu and beta rhythms over the sensorimotor cortices during mental tasks [7].

It is a statistical method for independent component analysis (ICA), which transforms observed multidimensional mixed signals into components that are statistically as independent as possible. It is a kind of blind source separation estimating the source components under unknown knowledge of sources. Compared with principal component analysis (PCA), which only ensures output patterns are uncorrelated, ICA makes certain their statistical independence. It has been applied extensively to remove artifacts for the analysis of EEG. The blind source separation could show neurophysiolgically and neuroanatomically meaningful neuronal components without the assumption of prior physic models [8]. In this study, an automatic method is proposed to remove the electrooculography (EOG) artifacts by means of the FastICA algorithm [9] and correlation coefficient.

It greatly affects the recognition rate for feature extraction is a very important issue. If extracted features are better, the higher classification accuracy can be expected. All kinds of feature extraction methods have been proposed. Among them, band power and AAR parameters are more popular [10-15]. Feature extraction based on band power estimation is usually obtained by computing their powers at several bands that are predominately

involved in mental tasks. The estimated band powers are then computed with their logarithm values as descriptive parameters for every channel, or estimated by averaging over them [10,11]. AAR models are also common in feature extraction of mental tasks [13,14]. The all-pole AAR model lends itself well to modeling EEG signals as filtered white noise with certain preferred energy bands. The EEG time series is fitted with an AAR model. In this study, phase-locking value (PLV) [16] together with discrete wavelet transform (DWT) is used to extract coherence features in multiscale for classification. The DWT is powerful in selecting features in multiresolution, and it is an efficient and structured approach to ERP representation [17,18]; whereas the PLV is advantageous in recognizing mental tasks possessing the phenomena of synchronization in brain activities.

It is a popular classifier for support vector machine (SVM) [19-24], which not only has a very steady theory in statistical learning, but guarantees to obtain the optimal decision function from a set of training data. It has the advantage that it can balance the accuracy and generalization by maximizing the performance of network as well as minimizing the complexity of learning machine. Accordingly, it is used for classification in this study.

To evaluate the performance of proposed system, EEG data without EOG artifact removal, spectral band and AR model features are implemented for comparison. The results show satisfactory classification accuracy for proposed automatic EOG artifact removal and wavelet-coherence features. This paper is organized as follows. In Section 2, data acquisition and analysis are presented. Section 3 describes experimental results and discussion. Finally, conclusion is given in Section 4.

2. **Materials and Methods.** A flowchart of proposed BCI system is illustrated in Figure 1 for single trial EEG classification. The procedure mainly consists of three steps: automatic noise elimination, feature extraction and classification. The artifacts and background noise of EEG data are eliminated automatically by ICA and surface Laplacian. The features are then extracted by the PLV from wavelet data. Finally, the SVM is used for the classification.

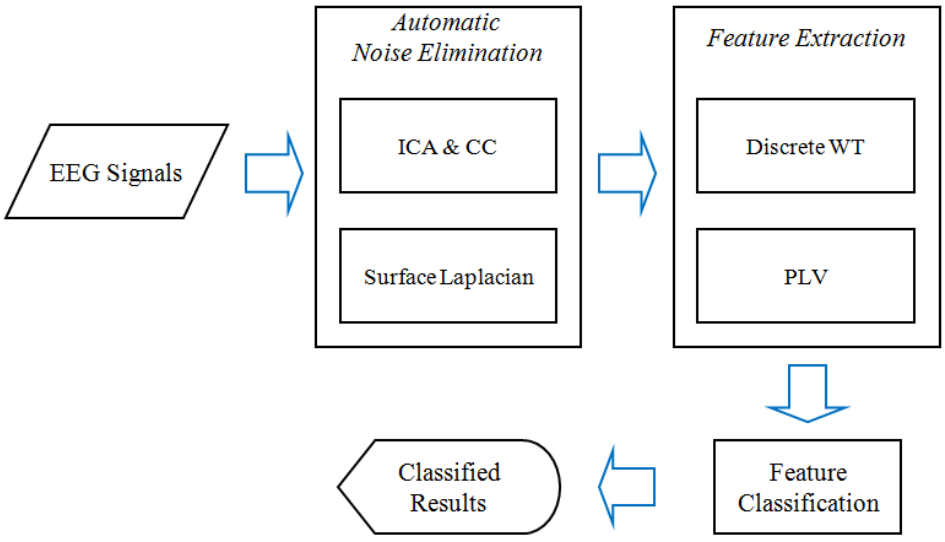

FIGURE 1. Flowchart of proposed BCI system. The system mainly consists of three procedures: automatic noise elimination, feature extraction and classification.

2.1. **Data acquisition.** EEG signals were recorded from six untrained subjects (five males and one female, two left-handed and four right-handed) in a shielded room using 13 silver/silver chloride electrodes, including ten scalp EEG channels (C3, C5, FC3, C1, CP3, C4, C2, C6, FC4, and CP4), two EMG channel for monitoring left and right muscle activity, and one channel on the forehead to record possible EOG artifacts and eye blinks during the experiment [25] as illustrated in Figure 2. All electrodes were referenced to the A1 lead at the left earlobe. Before being sampled at the rate of 256 Hz, the EEG data were filtered by an analog band-pass filter with cutoff frequencies at 0.5 Hz and 100 Hz, and amplified by a multiple of ten thousand. During the experiments, each subject was asked to perform two trials, which included left and right finger lifting in each test. Each trial was ten seconds in length, so it took twenty seconds in a test. For each lifting trial, the first 4 s was quiet and then an acoustic stimulus was given as a cue to signify the beginning of left finger lifting. At the same time, each subject was asked to execute a finger lifting. An example of a test is shown in Figure 3(a). We recorded sixty tests for each subject, and thus there were 120 trials for each subject. No trials were removed during the EEG data processing stage. Data segments for finger lifting were acquired from second -2 to second 2, where second 0 stands for the trigger of movement by detecting the peak EMG signal after linear envelope processing. (Only the data recorded between -2 and 2 s were considered to be event-related.)

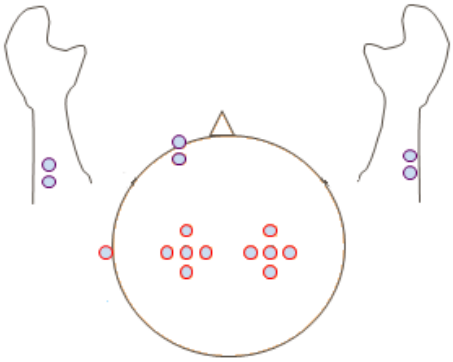

FIGURE 2. Electrode positions. EEG channels are measured according to the international standard 10-20 systems.

2.2. **Automatic noise elimination.**

2.2.1. *Independent component analysis and correlation coefficient.* ICA transforms observed multidimensional mixed signals into components that are as statistically independent from others as possible. It also resolves the blind source separation problem. In other words, the source components are calculated under almost no advance knowledge of the nature of sources. The PCA only ensures output patterns are uncorrelated, and the ICA guarantees they are statistically independent. Statistical independence needs that all high-order correlations are zero, whereas decorrelation only minimizes the second-order statistics. The ICA is applied to the blind source separation of EEG signals based on a reasonable assumption that EEG data acquired from multiple scalp electrodes are linear combinations of temporally independent components.

Each test was arranged into an $m \times n$ matrix, where m and n represent channel number and sample points. That is, the ith row contains acquired signals from ith channel, while the jth column means the sample at the jth time point across all channels. In this study, the FastICA algorithm [9] is used to remove the EOG artifacts because of its fast convergence. It eliminates the means of row vectors from the matrix and then uses

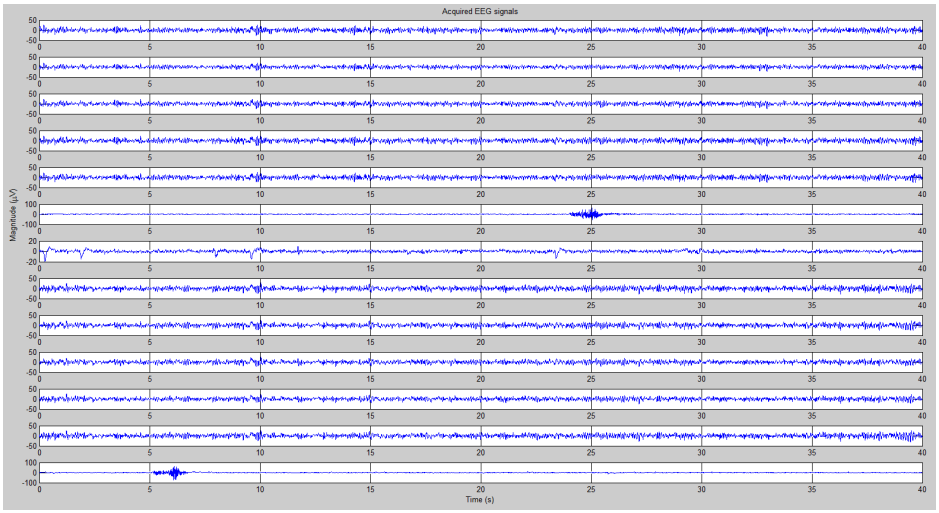

(a)

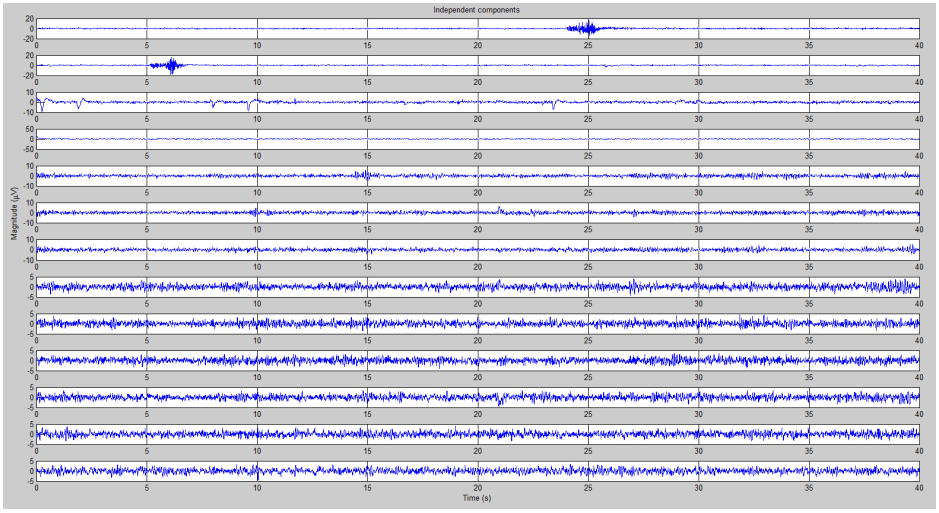

(b)

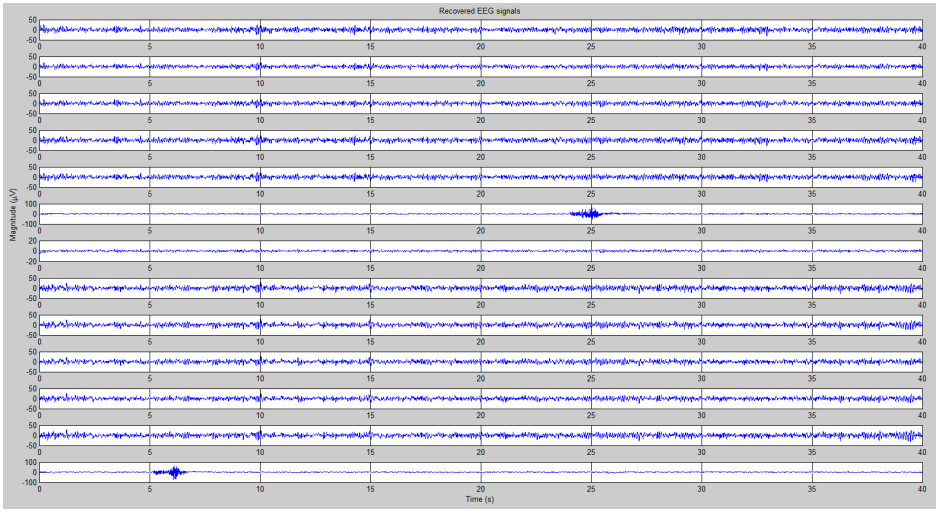

(c)

FIGURE 3. Procedure of automatic EOG artifact elimination. (a) Acquired EEG signals, (b) independent components and (c) recovered EEG signals without EOG artifacts.

a whitening procedure to transform the covariance matrix of zero-mean data into an identity matrix. Finally, it separates the whitened data into a set of components which are as mutually independent as possible.

In addition, a natural measure of similarity, the absolute value of correlation coefficient, between the EOG channel and estimated independent components is proposed to automatically eliminate the EOG artifacts. The independent component with maximal similarity, which must be larger than a predefined threshold, is regarded as pure EOG artifacts. After the removal of EOG artifacts, the EEG signals without EOG artifacts are recovered from remaining independent components. The procedure of automatic elimination of EOG artifacts is shown in Figure 3. In Figure 3(a), acquired (mixed) EEG signals are given. There are total 13 channels in the signals. The first five channels contain the signals of C3 group (C3, C5, FC3, C1, and CP3), while the signals of C4 group (C4, C2, C6, FC4, and CP4) are at channels 8-12. The REMG and LEMG signals are situated in channels 6 and 13 respectively, whereas the EOG artifacts are acquired from channel 7. Figure 3(b) shows independent components after performing the FastICA algorithm. In this example, the maximum of similarity between the EOG channel and independent components is 0.8955 and this component is located at third channel of independent components. The recovered EEG signals without EOG artifacts are shown in Figure 3(c). We can observe that the EOG artifacts have been eliminated clearly and only EEG signals with low magnitude remain in EOG channel, which is rational in the explanations.

2.2.2. *Surface Laplacian.* There are greatly differences between EEG signals and Non-EEG noise in both topographical and frequency characteristics. The mu and beta rhythms of the EEG are those components with frequencies distributed between 8-30 Hz and located over the sensorimotor cortex. EOG signals are maximal at low frequencies ($<$ 5 Hz) and are prominently situated over the anterior head regions. Accordingly, an appropriate filtering method can increase the signal-to-noise ratio by reducing non-EEG noise. The surface Laplacian filter is a simple but effective filtering method [26]. It calculates the second derivative of the spatial voltage distribution for a selected electrode. It is a high-pass spatial filter that enhances localized activities and reduces background noise. This filter is achieved by subtracting the average potential of a set of surrounding electrodes from the electrode of interest,

$$V_i^{Lap} = V_i - \frac{1}{N} \sum_{j \in S_i} V_j \tag{1}$$

where V_i represents the potential between the ith electrode and the reference A1, and S_i and N stand for the set of electrodes surrounding the ith electrode and the number of surrounding electrodes, respectively. The distance between the selected electrode and its surrounding electrodes demonstrates the characteristic of surface Laplacian filtering that the greater the distance, the greater the insensitivity to highly localized potentials. The 4-s window was acquired from the finger-lifting trial with its center standing for the trigger of movement.

2.3. **Feature extraction.** Before the classification, feature extraction is performed on the event-related windows rather than directly classifying the native EEG data without feature extraction. It greatly affects the recognition rate for feature extraction. That is, the better the extracted features, the higher the performance we can expect.

2.3.1. *Discrete wavelet transform.* We first band-pass filtered the windows to the wide frequency range that contains all mu and beta rhythmic components using a Butterworth

band-pass filter. The Daubechies discrete wavelet transform (DWT) [27-36] is then performed on the filtered windows. The reason we choose the Daubechies wavelet is due to the special characteristic that Daubechies family wavelets are compactly supported with extreme phase and highest number of vanishing moments for a given support width.

Multiresolution analysis decomposes a signal into numerous details at various resolutions, where each resolution represents a class of distinct physical characteristics within the signal. More specifically, a signal is characterized with the formulation by decomposing it into sub-bands, and each sub-band can be treated individually based on its characteristics. Multiresolution representation of filtered event-related windows is achieved by Daubechies DWT. The event-related window W for each trial is represented in terms of the DWT as

$$W(x) = \sum_{k=-\infty}^{\infty} S_J(k)\, 2^{J/2}\phi\left(2^J x - k\right) + \sum_{j=1}^{J}\sum_{k=-\infty}^{\infty} D_j(k) 2^{j/2}\psi\left(2^j x - k\right) \tag{2}$$

where $S_J(k)$ and $D_j(k)$ represent the approximation and detail spaces of W, respectively, and $2^{J/2}\phi\left(2^J x - k\right)$ and $2^{j/2}\psi\left(2^j x - k\right)$ denote the dilated and translated versions of the scaling function $\phi(x)$ and wavelet function $\varphi(x)$, respectively. The event-related window W is then decomposed into individual subbands S_J, D_J, ..., and D_1.

2.3.2. *Coherence and phase-locking value.* A variety of approaches have been proposed to measure the synchronization of two signals. The coherence [37] is popular in analyzing EEG signals. It is derived from the cross-spectrum of two time-series signals. More specifically, the Fourier transform of a signal $x_i(t)$ is represented in terms of its amplitude r_i and phase θ_i as,

$$X_i(f) = r_i \exp(j\theta_i) \tag{3}$$

The cross-spectrum of two signals are then defined as,

$$CS_{ij}(f) = \langle r_i r_j \exp(j\Delta\theta)\rangle \tag{4}$$

where $\langle\rangle$ represents the expectation operator, and $\Delta\theta$ denotes the phase difference between these two signals. The complex coherence is the cross-spectrum normalized with the two spectra of corresponding signals,

$$CC_{ij}(f) = \frac{\langle r_i r_j \exp(j\Delta\theta)\rangle}{\sqrt{\langle r_i^2\rangle}\sqrt{\langle r_j^2\rangle}} \tag{5}$$

The coherence is then obtained by calculating the absolute value of complex coherence,

$$C_{ij}(f) = \left|\frac{\langle r_i r_j \exp(j\Delta\theta)\rangle}{\sqrt{\langle r_i^2\rangle}\sqrt{\langle r_j^2\rangle}}\right| \tag{6}$$

In addition, the PLV is another popular term used to measure the synchrony of two signals in EEG studies recently [16,38,39]. It is defined as,

$$PLV_{ij} = |\langle \exp(j\Delta\theta)\rangle| \tag{7}$$

It is similar to the coherence. That is, the PLV only contains the phase difference between two signals, but their amplitudes are not included in the PLV. Since only the synchronization of phases is evaluated, it may be a more suitable measure to investigate

the phenomena of synchronization in EEG signals [39]. In single-trial applications, the coherence and PLV are calculated by carrying out the average process over time,

$$C_{ij}(f) = \frac{1}{T_2 - T_1} \left| \sum_{t=T_1}^{T_2} \frac{r_i(t) r_j(t) \exp(j\Delta\theta(t))}{\sqrt{r_i(t)^2}\sqrt{r_j(t)^2}} \right| \tag{8}$$

$$PLV_{ij} = \frac{1}{T_2 - T_1} \left| \sum_{t=T_1}^{T_2} \exp(j\Delta\theta(t)) \right| \tag{9}$$

where $\Delta\theta(t)$ represents the difference of instantaneous phase at time sample t. In this study, the coherence and PLV are calculated to obtain the phase synchronization from the subbands obtained by the DWT. They are then averaged over time samples of subbands of event-related windows.

2.4. **Classification.** It is difficult to construct conventional neural networks since it is necessary to choose appropriate number of hidden layers and neurons to approximate the function in question to the desired accuracy. If the number in the network is more, it may over-fit the training data and results in very poor generalization. The SVM [19] not only has a very steady theory in statistical learning, but guarantees to obtain the optimal decision function from a set of training data. The concept of SVM is that the data can be linearly separated from two sets through a hyperplane if a nonlinear mapping of high-dimensional feature space is appropriately chosen. In addition, its advantage is to balance the accuracy and generalization by maximizing the performance of network as well as minimizing the complexity of learning machine at the same time. The main idea of SVM is to construct a hyperplane as the decision surface in such a way that the margin of separation between positive and negative examples is maximized. The SVM optimization problem is

$$\begin{aligned} &\min_w \frac{1}{2} w^T w + C \sum_{i=1}^{N} \xi_i \\ &\text{subject to} \xi_i \geq 0, \ \forall i, \ \text{and} \ d_i \left(w^T x_i + b \right) \geq 1 - \xi_i, \ \forall\, i = 1, 2, \ldots, N \end{aligned} \tag{10}$$

where $g(x) = w^T x + b$ represents the hyperplane, w is the weighting vector, b is the bias term, x is the training vector with label d, C is the weighting constant, and ξ is the slack variable. It is then transformed into a convex quadratic dual problem. The discriminant function with optimal w and b, $g(x) = w_o^T x + b_o$, posterior to the optimization form becomes

$$g(x) = \sum_{i=1}^{N} \alpha_i d_i K(x, x_i) + b_o \tag{11}$$

where α is a Lagrange multiplier and $K(x, x_i)$ is a kernel function. Generally, appropriate kernel functions [19] are the polynomial kernel function $K(x_i, x_j) = \left(x_i^T x_j + 1\right)^p$ and the radial basis function (RBF) kernel function $K(x_i, x_j) = \exp\left((-1/2\sigma^2) \ \|x_i - x_j\|^2\right)$.

3. Results and Discussion.

3.1. **Procedure of automatic EOG artifact elimination.** The process of automatic EOG artifact removal is demonstrated in Figure 3. Figure 3(a) shows raw EEG signals, which involve C3 and C4 group, EOG artifacts, and LRMG and REMG signals. The independent components of ICA decomposition are shown in Figure 3(b). In this case, independent component maximally similar to the EOG signal is situated at third channel. The other independent components are similar to EEG signals and some noise. The

recovered EEG signals are shown in Figure 3(c), after the third independent component is eliminated. We can observe that EOG artifacts in EOG channel have been completely removed. The left signals in this channel are EEG signals with low magnitude. It is quite reasonable because original EOG signals are mixed signals, which may contain some little EEG and EMG signals, besides EOG artifacts. Moreover, the EOG artifacts that are mixed into the EEG signals of C3 and C4 group have been also removed clearly. It reveals that the removal can increase the discriminant stability of EEG data by automatically eliminating the influence of EOG artifacts.

3.2. **Performance and statistical evaluation for EOG artifact elimination.** The classification tests for EEG data are carried out using five-fold cross validation in this study. More specifically, the dataset for each subject is divided into five subsets, and the following procedure is repeated five times. Each time, one of the five subsets is used as the test set and the other four are used as training set. The average recognition rate is immediately evaluated across all five folds. To verify the effectiveness of proposed automatic EOG artifact removal, we compare the classification accuracy between without and with automatic EOG artifact removal under the wavelet-coherence features and SVM classifier. The comparisons of classification accuracy are listed in Table 1. The results show that the average accuracy for without EOG artifact removal is 73.6%, while that for with EOG artifact removal increases to 79.8%. Hence, it indicates that the proposed automatic EOG artifact removal can improve the overall performance in EEG classification. In other words, after eliminating EOG artifacts, classification accuracy increases for all subjects.

TABLE 1. Comparison of classification accuracy between without and with EOG artifact elimination

Classification Accuracy	Subj#1	Subj#2	Subj#3	Subj#4	Subj#5	Subj#6	Average
w/o EOG artifact removal	76.7%	77.9%	73.0%	77.7%	67.9%	68.1%	73.6%
EOG artifact removal	81.6%	84.4%	77.8%	86.7%	73.8%	74.6%	79.8%

Moreover, two-way ANOVA is performed to validate if the results of automatic EOG artifact removal are significantly different or not. The results indicate that the performance improvement is significant (p-value 0.0002). Accordingly, automatic EOG artifact removal can efficiently eliminate the EOG artifacts to further improve the performance.

3.3. **Performance and statistical evaluation of features.** Feature extraction greatly affects the success of classification. In other words, when extracted features are better, we could obtain higher classification accuracy. Hence, combined with wavelet transform, the PLV is used to extract coherence features in multiscale for classification. It is because the DWT is an efficient and structured approach in ERP representation. In addition to multiscale characteristics, the features also contain important coherence information. Moreover, all kinds of feature extraction methods have been proposed. Among them, the spectral band and AR model are common, so they are implemented in comparison with the proposed features.

An experiment is performed for evaluating the performance of proposed features. Table 2 shows the comparison of classification accuracy among spectral band, AR model and wavelet-coherence features under the EOG artifact removal and SVM classifier. These three features are applied to the same EOG artifact removal and classifier. In other words, the listed values demonstrate only the deviations of performance among different features. Overall, the average recognition rate for spectral band and AR model features is about 71%, whereas using wavelet-coherence as features yields the best average rate

TABLE 2. Comparison of classification accuracy among spectral band, AR model and wavelet-coherence features

Classification Accuracy	Subj#1	Subj#2	Subj#3	Subj#4	Subj#5	Subj#6	Average
Spectral band	72.1%	74.4%	71.8%	77.4%	67%	64.7%	71.2%
AR model	67.3%	72.9%	72.1%	76.7%	66.8%	67.2%	70.5%
Wavelet-coherence features	81.6%	84.4%	77.8%	86.7%	73.8%	74.6%	79.8%

(79.8%), the difference being about 9%. In addition, we observe that the proposed features give the best results for all subjects. It indicates that the proposed features can obtain the best performance in EEG classification.

Moreover, two-way ANOVA and multiple comparison tests are performed to verify if the comparison among features is significantly different. The results indicate that the differences between "spectral band and wavelet-coherence features" and "AR model and wavelet-coherence features" are significant (p-values 0.0001 and 0.0009). That is, the wavelet-coherence features are significantly better than other two features in BCI applications.

4. **Conclusion.** A BCI system has been proposed for single-trial EEG classification in this study. It consists of automatic noise elimination, feature extraction and classification, and is present for the left and right MI data analysis. The EOG artifacts and background noise are removed automatically, which can increase the performance. The features are extracted from wavelet data by coherence, which gives the phase synchronization of mental tasks, and then classified by means of the SVM. Experimental results denote the proposed methods are better than those EEG data without EOG artifact removal, spectral band and AR model features in classification accuracy. In future works, we will develop some more powerful artifact-removal methods and features to further enhance the performance.

Acknowledgements. The author would like to express his sincere appreciation for grants from NSC101-2320-B-038-001 and NSC101-2221-E-194-066, National Science Council, Taiwan.

REFERENCES

[1] C. R. Hema, M. P. Paulraj, R. S. Y. Nagarajan and A. H. Adom, Brain machine interface: A comparison between fuzzy and neural classifiers, *International Journal of Innovative Computing, Information and Control*, vol.5, no.7, pp.1819-1827, 2009.

[2] L. Parra, C. Alvino, A. C. Tang, B. A. Pearlmutter, N. Yeung, A. Osman and P. Sajda, Linear spatial integration for single trial detection in encephalography, *NeuroImage*, vol.7, no.1, pp.223-230, 2002.

[3] T. Yamaguchi, K. Nagata, P. Q. Truong, M. Fujio and K. Inoue, Pattern recognition of EEG signal during motor imagery by using SOM, *International Journal of Innovative Computing, Information and Control*, vol.4, no.10, pp.2617-2630, 2008.

[4] W. Y. Hsu and Y. N. Sun, EEG-based motor imagery analysis using weighted wavelet transform features, *Journal of Neuroscience Methods*, vol.167, no.2, pp.310-318, 2009.

[5] Z. Zhang, H. Ikeuchi, N Saiki, T. Imamura, T. Miyake1, H. Toda and S. Horihata, Fast wavelet instantaneous correction and its application to abnormal signal detection, *International Journal of Innovative Computing, Information and Control*, vol.4, no.10, pp.2697-2710, 2008.

[6] W. Y. Hsu, EEG-based motor imagery classification using neuro-fuzzy prediction and wavelet fractal features, *Journal of Neuroscience Methods*, vol.189, no.2, pp.295-302, 2010.

[7] G. R. Muller-Putz, D. Zimmermann, B. Graimann, K. Nestinger, G. Korisek and G. Pfurtscheller, Event-related beta EEG-changes during passive and attempted foot movements in paraplegic patients, *Brain Research*, vol.1137, pp.84-91, 2007.

[8] A. C. Tang, B. A. Pearlmutter, M. Zibulevsky and S. A. Carter, Blind source separation of multichannel neuromagnetic responses, *Neurocomputing*, vol.32-33, pp.1115-1120, 2000.

[9] A. Hyvarinen, J. Karhunen and E. Oja, *Independent Component Analysis*, John Wieley & Sons, Inc., New York, 2001.
[10] F. V. Nelwamondo, T. Marwala and U. Mahola, Early classifications of bearing faults using hidden markov models, Gaussian mixture models, mel-frequency cepstral coefficients and fractals, *International Journal of Innovative Computing, Information and Control*, vol.2, no.6, pp.1281-1299, 2006.
[11] Z. Zhang and Y. Zhao, Multiple description image coding based on fractal, *International Journal of Innovative Computing, Information and Control*, vol.3, no.6(B), pp.1615-1623, 2007.
[12] Z. Zhang and Y. Zhao, Improving the performance of fractal image coding, *International Journal of Innovative Computing, Information and Control*, vol.2, no.2, pp.387-398, 2006.
[13] Z. Zhang, H. Ikeuchi, H. Toda, T. Miyake, T. Imamura, H. Ishii and S. Horihata, Wavelet and applying it in abnormal signal detection, *International Journal of Innovative Computing, Information and Control*, vol.4, no.4, pp.1009-1022, 2008.
[14] F.-X. Yu, J.-Y. Su, Z.-M. Lu, P.-H. Huang and J.-S. Pan, Multi-feature based fire detection in video, *International Journal of Innovative Computing, Information and Control*, vol.4, no.8, pp.1987-1993, 2008.
[15] K.-H. Huarng, T. H.-K. Yu and T.-T. Kao, Analyzing structural changes using clustering techniques, *International Journal of Innovative Computing, Information and Control*, vol.4, no.5, pp.1195-1201, 2008.
[16] F. Censi, G. Calcagnini, S. Lino, S. R. Seydnejad and R. I. Kitney, Transient phase locking patterns among respiration, heart rate and blood pressure during cardiorespiratory synchronisation in humans, *Med. Bio. Eng. Comput.*, vol.38, no.4, pp.416-426, 2000.
[17] W. Y. Hsu, C. C. Lin, M. S. Ju and Y. N. Sun, Wavelet-based fractal features with active segment selection: Application to single-trial EEG data, *Journal of Neuroscience Methods*, vol.163, no.1, pp.145-160, 2007.
[18] W. Y. Hsu, W. F. P. Poon and Y. N. Sun, Automatic seamless mosaicing of microscopic images: Enhancing appearance with color degradation compensation and wavelet-based blending, *Journal of Microscopy-Oxford*, vol.231, no.3, pp.408-418, 2008.
[19] B. E. Boser, I. M. Guyon and V. Vapnik, A training algorithm for optimal margin classifiers, *Proc. of the 5th Annu. Workshop on Computational Learning Theory*, pp.144-152, 1992.
[20] N. Shimo, S. Pang, N. Kasabov and T Yamakawa, Curiosity-driven multi-agent competitive and cooperative LDA learning, *International Journal of Innovative Computing, Information and Control*, vol.4, no.7, pp.1537-1552, 2008.
[21] H. Zhu, H. Kai, K. Eguchi, Z. Guo and J. Wang, Application of BPNN in classification of time intervals for intelligent intrusion detection decision response system, *International Journal of Innovative Computing, Information and Control*, vol.4, no.10, pp.2483-2491, 2008.
[22] K. Shinkai, Decision analysis of fuzzy partition tree applying fuzzy theory, *International Journal of Innovative Computing, Information and Control*, vol.4, no.10, pp.2581-2594, 2008.
[23] H.-C. Liu, J.-M. Yih, W.-C. Lin and T.-S. Liu, Fuzzy C-means algorithm based on PSO and Mahalanobis distance, *International Journal of Innovative Computing, Information and Control*, vol.5, no.12(B), pp.5033-5040, 2009.
[24] K. Zou, J. Hu, W. Li and L. Yu, FCM clustering based on ant algorithm and its application, *International Journal of Innovative Computing, Information and Control*, vol.5, no.12(B), pp.4819-4824, 2009.
[25] H. Jasper, The ten-twenty electrode system of the international federation, *Electroenceph. Clin. Neurophysiol.*, vol.10, pp.371-375, 1958.
[26] D. J. McFarland, L. M. McCane, S. V. David and J. R. Wolpaw, Spatial filter selection for EEG-based communication, *Electroencephalogr. Clin. Neurophysiol.*, vol.103, pp.386-394, 1997.
[27] I. Daubechies, *Ten Lectures on Wavelets, CBMS-NSF Lecture Notes*, SIAM, 1992.
[28] W. Y. Hsu, Analytic differential approach for robust registration of rat brain histological images, *Microscopy Research and Technique*, vol.74, no.6, pp.523-530, 2011.
[29] W. Y. Hsu, EEG-based motor imagery classification using enhanced active segment selection and adaptive classifier, *Computers in Biology and Medicine*, vol.41, no.8, pp.633-639, 2011.
[30] W. Y. Hsu, Continuous EEG signal analysis for asynchronous BCI application, *International Journal of Neural Systems*, vol.21, no.4, pp.335-350, 2011.
[31] W. Y. Hsu, Application of multiscale amplitude modulation features and FCM clustering to brain-computer interface, *Clinical EEG and Neuroscience*, vol.43, no.1, pp.32-38, 2012.
[32] W. Y. Hsu, Fuzzy hopfield neural network clustering for single-trial motor imagery EEG classification, *Expert Systems with Applications*, vol.39, no.1, pp.1055-1061, 2012.

[33] W. Y. Hsu, Enhanced active segment selection for single-trial EEG classification, *Clinical EEG and Neuroscience*, vol.43, no.2, pp.87-96, 2012.

[34] W. Y. Hsu, C. H. Lin, H. J. Hsu, P. H. Chen and I. R. Chen, Wavelet-based envelope features with automatic EOG artifact removal: Application to single-trial EEG data, *Expert Systems with Applications*, vol.39, no.3, pp.2743-2749, 2012.

[35] W. Y. Hsu, Registration accuracy and quality of real-life images, *PLoS ONE*, vol.7, no.7, e40558, 2012. DOI:10.1371/journal.pone.0040558.

[36] W. Y. Hsu, Application of competitive hopfield neural network to brain-computer interface systems, *International Journal of Neural Systems*, vol.22, no.1, pp.51-62, 2012.

[37] P. L. Nunez, R. Srinivasan, A. F. Westdorp, R. S. Wijesinghe, D. M. Tucker, R. B. Silberstein and P. J. Cadusch, EEG coherency I: Statistics, reference electrode, volume conduction, laplacians, cortical imaging, and interpretation at multiple scales, *Electroencephalogr. Clin. Neurophysiol.*, vol.103, pp.499-515, 1997.

[38] C. C. Chen, W. Y. Hsu and S. H. Chiu, An efficient algorithm for point set registration using analytic differential approach, *IEICE Transactions on Information and Systems*, vol.E93-D, no.11, pp.3100-3107, 2010.

[39] H. Carlqvist, V. V. Nikulin, J. O. Strömberg and T. Brismar, Amplitude and phase relationship between alpha and beta oscillations in the human electroencephalogram, *Med. Bio. Eng. Comput.*, vol.43, no.5, pp.599-607, 2005.